Linear Modelling of Series FACTS Devices in Power System Operation Models

Xinyang Rui[1], Mostafa Sahraei-Ardakani[1*], Thomas R. Nudell[2]
[1]Department of Electrical and Computer Engineering, University of Utah, Salt Lake City, UT 84112, USA
[2]Smart Wires Inc., Union City, CA 94587, USA

Corresponding author: Mostafa Sahraei-Ardakani
Address: 50 S Central Campus Dr., MEB 2218, Salt Lake City, UT, 84112
e-mail: mostafa.ardakani@utah.edu

Funding:
This research was funded by the National Science Foundation grant # 1756006.

Conflict of Interest:
Dr. Nudell works for Smart Wires Inc., a developer of modular flexible ac transmission system devices.

Permission to reproduce materials from other sources:
None

Data Availability Statement:
The data that support the findings of this study are openly available in:
'ACTIVSg2000: 2000-bus synthetic grid on footprint of Texas' at https://electricgrids.engr.tamu.edu/electric-grid-test-cases/activsg2000/, reference number [55];
'Power System Test Case Archive - Reliability Test System (RTS)-1996' at http://labs.ece.uw.edu/pstca/rts/pg_tcarts.htm, reference number [56];
'SmartValve™ v1.04 Spec Sheet' at https://www.smartwires.com/download/20801/, reference number [57];
'Power Systems Test Case Archive - 14 Bus Power Flow Test Case' at https://labs.ece.uw.edu/pstca/pf14/pg_tca14bus.htm, reference number [58];
'Description of Case 14' at https://matpower.org/docs/ref/matpower5.0/case14.html, reference number [59].
'A Data Sheet for IEEE 14 Bus System' at https://www.academia.edu/7781632/A_DATA_SHEETS_FOR_IEEE_14_BUS_SYSTEM, reference number [60].

Linear Modelling of Series FACTS Devices in Power System Operation Models

Xinyang Rui[1], Mostafa Sahraei-Ardakani[1*], Thomas R. Nudell[2]

[1]Department of Electrical and Computer Engineering, University of Utah, Salt Lake City, UT 84112, USA
[2]Smart Wires Inc., Union City, CA 94587, USA
[*]mostafa.ardakani@utah.edu

Abstract: This paper presents injection-shift-factor-based linear modelling for various types of series flexible ac transmission system (FACTS) devices within the DC power flow framework. The presented models allow FACTS devices to be properly integrated in current operation and planning software tools, which is key to harnessing the power flow capabilities provided by FACTS technology. Although recent literature has attempted to develop linear models for FACTS devices, the existing models do not accurately reflect the actual operating range for many FACTS devices. Compared to the existing models, the modelling approach presented in this paper reflects the principle of operation of each type of series FACTS device in adjusting transmission line reactance. Through mathematical derivation, linear constraints for FACTS operation are formulated, which are used to formulate power system operation models. The formulated problems are then analysed through simulation studies on various test systems. The results highlight the significant computational efficiency improvements provided by linear FACTS modelling in DC-based operation models.

Nomenclature

Indices and sets

i, j, n	Index of buses
ij	Index of transmission line from bus i to j
t	Index of time
g	Index of generators
N	Set of all buses in the network
T	Set of time periods
G	Set of all generators in the network
$G(i)$	Set of generators located at bus i
K_{F}	Set of transmission lines equipped with FACTS devices
$N^{+}(i)$	Set of buses that has a transmission line connected "to" bus i
$N^{-}(i)$	Set of buses that has a transmission line connected "from" bus i

Variables

$\tilde{b}_{ij}$	Susceptance of transmission line ij with FACTS deployed
f_{ij} ($f_{ij,t}$)	Active power flow through transmission line ij (at time t)
$\tilde{f}_{ij}$ ($\tilde{f}_{ij,t}$)	Partial power flow not including FACTS injection through transmission line ij (at time t)
θ_i (θ_{it})	Voltage angle at bus i (at time t)
Δx_{ij} ($\Delta x_{ij,t}$)	Effective reactance injection of FACTS devices on transmission line ij (at time t)
Δf_{ij} ($\Delta f_{ij,t}$)	FACTS power injection on transmission line ij (at time t)
Δb_{ij}	Susceptance change on transmission line ij
I_{ij}	Current on transmission line ij
N_{ij}^{FACTS}	Number of M-FACTS devices installed on transmission line ij
$\dot{V}_i$	Voltage phasor of bus i
$\dot{V}_{ij}^{\mathrm{se}}$	FACTS series voltage injection phasor for transmission line ij
$\dot{V}_i^{\mathrm{sh}}$	UPFC shunt voltage injection phasor for transmission bus i
$\dot{I}_{ij}$	Current phasor of transmission line ij
φ_{ij} ($\varphi_{ij,t}$)	Phase angle of UPFC voltage injection on transmission line ij (at time t)
x_{TCSC}	TCSC reactance injection
z_{ij} ($z_{ij,t}$)	Binary variable representing flow direction of transmission line ij (at time t)
p_g (p_{gt})	Active power output of generator g (at time t)
ψ_i (ψ_{it})	Power injection at bus i (at time t)
u_g (u_{gt})	Unit commitment variable of generator g (at time t)
v_g (v_{gt})	Start-up variable of generator g (at time t)

Parameters

b_{ij}	Pre-injection susceptance of transmission line ij
$b_{ij}^{\min}$, $b_{ij}^{\max}$	Minimum and maximum susceptance of transmission line ij equipped with FACTS
x_{ij}	Reactance of transmission line ij
$V_{ij}^{\max}$	Maximum voltage injection of SSSC or UPFC devices on transmission line ij
$I_{ij}^{\max}$	Maximum current on transmission line ij
$I^{\min}$	Minimum current to power up FACTS devices
$f^{\min}$	Minimum flow to power up FACTS devices
$\overline{V}$	Maximum voltage injection of a single M-SSSC device
$x_{\mathrm{TCSC}}^{\min}$, $x_{\mathrm{TCSC}}^{\max}$	Minimum and maximum reactance injection of TCSC devices
c_g	Marginal cost of generator g
Φ_{ij}^{n}	Injection shift factor associating bus n to transmission line ij
$f_{ij}^{\max}$	Capacity of transmission line ij
d_i (d_{it})	Demand on bus i (at time t)
$N_{ij}^{\max}$	Maximum number of M-FACTS allowed to

	be deployed on transmission line ij
$N^{\max}$	Total number of available M-FACTS devices
k_g	No-load cost of generator g
s_g	Start-up cost of generator g
R_g^+, R_g^-	Maximum hourly ramp rate of generator g
UT_g, DT_g	Minimum up and down time of generator g
M	A very large positive number

1. Introduction

The transmission system in the United States is outdated and needs to be upgraded [1]. High congestion costs in many parts of the US power grid is a strong economic signal for this need [2]. A robust transmission network is also central to reliability of the electric power grid [3]. Insufficient transfer capability leads to congestion in the transmission network, which may result in violations of network security limits [4]. Transfer capability enhancement, thus, improves economic efficiency and reliability of the bulk power network. Moreover, enhancing transfer capability facilitates penetration of higher levels of renewable generation in power systems. Renewable energy penetration is expected to rapidly grow and reach 42% of the total energy mix in the U.S. by 2050 [5]. However, congestion in the transmission network hinders the delivery of high levels of renewable generation [6], causing problems such as wind energy curtailment.

Transfer capability can be enhanced through construction of new transmission lines. However, the process of building new lines is lengthy and costly due to social and environmental issues, as well as new challenges such as market deregulation [7]. A faster alternative is improving the utilisation of the existing transmission network, which can be achieved through power flow control [8]. Note that the increase in transfer capability over the existing grid can be as large as 30% [8], [9]. One technology that enables power flow control is flexible ac transmission systems (FACTS). FACTS devices facilitate rerouting of power flow to avoid transmission bottlenecks and congested lines, which results in enhanced transfer capability and increased dispatch of cheaper generators. As an example, it is shown in [10] that the power flow control capabilities of FACTS devices can effectively reduce wind curtailment and reduce total generation cost. FACTS devices that are capable of effectively alter apparent impedance of transmission lines can be deployed for active power flow control. For the rest of this paper, the term "FACTS" is used to specifically refer to these types of devices. The impedance control can be either through direct addition of a controlled series impedance or injection of a controlled voltage, which emulates a controllable variable impedance.

While FACTS technology is a few decades old and there are numerous studies on a wide range of its benefits, the benefits can only be fully harnessed if FACTS devices are properly modelled in power system operation and planning models. Otherwise, the setpoint of these devices cannot be adjusted dynamically based on the state of the system, leading to some level of underperformance. Unfortunately, due to the computational complexity of including FACTS devices in operation and planning software tools, this integration has not yet occurred, resulting in under-materialised benefits of current FACTS installations [11-13]. Moreover, the widely used representation of FACTS operating range in DC power flow in recent studies are inaccurate for many FACTS devices. In the following subsection, we present a review of the existing model and the usage of it in the literature.

1.1. Review of existing models for the operating range of series FACTS in DC-based operation models

Independent system operators (ISOs) use DC-based market operations because of its robustness and operators' confidence in the quality of the solution [14]. Energy and market management system (EMS/MMS) software tools use one or another form of DC power flow models [15], [16]. Therefore, to enable integration of FACTS devices in EMS/MMS software tools, they should be modelled and integrated in DC-based operation models, often based on DC optimal power flow (DCOPF) and unit commitment (UC). The linearisation in DC power flow is mostly on power flow equations, which results in a computationally tractable formulation.

With FACTS devices, line reactance or susceptance can be controlled. Therefore, susceptance of transmission lines equipped with FACTS should be represented as a variable, as is shown in the b-θ DC power flow equation in (1).

$$f_{ij} = \tilde{b}_{ij}\left(\theta_j - \theta_i\right) \tag{1}$$

An early study on the representation of FACTS in DCOPF models the operating range of FACTS devices that provide series reactance adjustment as a variable with constant variation bounds [17], as is shown in (2).

$$b_{ij}^{\min} \le \tilde{b}_{ij} \le b_{ij}^{\max} \tag{2}$$

In this paper, we refer to such modelling approach as the *variable-susceptance* model. It has alternative reactance-based representations in different studies that are essentially equivalent. Note that with (2), (1) is a nonlinear equation, due to the bilinear terms $\tilde{b}_{ij}\theta_j$ and $\tilde{b}_{ij}\theta_i$. The nonlinearity makes optimisation problems much more computationally demanding. Additionally, nonlinear models are not compatible with existing EMS/MMS software tools. Thus, linearisation of (1) is essential for proper integration of FACTS devices in operation software tools. A number of recent research papers have focused on effectively reformulating (1) and (2) to linear or mixed-integer linear constraints [11-13], [18-20].

The variable-susceptance model of FACTS operating range is used in [11-13], where both the thyristor controlled series compensator (TCSC) and the unified power flow controller (UPFC) are presented as examples, where the model can be applied. However, according to the analysis in this paper, while the variable-susceptance model is an accurate representation for the TCSC, it cannot accurately reflect the operating range of UPFC devices because of the aforementioned difference in the impedance control methods. In [20], the type of series FACTS device is not clearly specified, when applying the variable-susceptance model. Similar issues reside in [21-23], where DC-based models with the distributed FACTS (D-FACTS) included are studied. However, the variable-susceptance model is used for modelling the operating range of D-FACTS devices, without specifying the type of FACTS technology.

In summary, the following gaps exist in the literature:

- Several studies simply apply the variable-susceptance model on devices, where the model cannot accurately reflect the impedance control method. As mentioned previously, depending on the type of FACTS device, different power electronic circuits are used to alter the apparent line impedance. The impacts are similar, yet the operating range of effective reactance injection may vary significantly, with some being highly nonlinear. The variable-susceptance model cannot accurately represent the true operating range of many FACTS devices.
- The variable-susceptance model is used as a general model in previous research without specifying the type of FACTS technology.
- The existing literature on the static synchronous series compensator (SSSC), the magnetic energy recovery switch (MERS), and the UPFC are by in large AC-based models [24-26]. Efficient and accurate linear modelling in DC-based software tools do not exist.
- A linear model for the emerging lightweight and compact modular FACTS (M-FACTS) devices is desirable.

1.2. Contributions

This paper fills the aforementioned gaps in the existing literature by making the following contributes.

- This paper derives accurate and computationally efficient models for various types of series FACTS devices. The models, developed here, reflect the specific characteristics of different devices in operation. The models are formulated as linear or mixed-integer linear constraints, to enable appropriate integration with DCOPF and UC, while achieving computational tractability, allowing smooth integration within the existing operation and planning software tools. Specifically, this paper models the following FACTS devices: the SSSC, the MERS, the UPFC, and the TCSC.
- Operation and planning and models for the emerging lightweight and compact modular FACTS (M-FACTS) devices, particularly the modular SSSC (M-SSSC), are also included.
- The mathematical derivation for each type of device, in this paper, is based on the usage of injection shift factors (ISFs). The impact of series compensation is modelled as power injections, with careful attention to the differences between each category of devices. ISF-based operation model formulations with each category of FACTS are presented at the end of the paper, which can serve as a reference for power system researchers that are interested in FACTS modelling, operation, and planning problems.
- The formulated problems are studied through simulations using the Texas 2000-bus system, the RTS-96 system, and the IEEE 14-bus system. The results show the computational efficiency of linear FACTS modelling, while also providing numerical verification for our mathematical derivations.

To the best of our knowledge, this is the first comprehensive study on efficient and accurate modelling of FACTS devices using ISFs in DC-based operation models.

1.3. Paper layout

The rest of this paper is organised as follows: the derivation leading to formulation of power flow control constraints for each type of FACTS is presented in Section 2. Note that the term "power flow control constraints" is used to refer to the constraints that are directly related to FACTS series compensation. They include the constraints reflecting the operating range of FACTS, as wells the power flow equation with consideration of FACTS reactance adjustments. Formulations of DCOPF and UC problems with both linear and nonlinear FACTS modelling are presented in Section 3. In Section 4, the results of simulation studies are provided and analysed. Finally, a conclusion is drawn in Section 5.

2. Linear FACTS Modelling

In this section, we present the mathematical modelling of effective reactance injection operating range of FACTS devices including SSSC, M-SSSC, UPFC, TCSC, and MERS. The focus of this section is on (i) derivation of accurate models, based on the principles of operation for each type of FACTS device to adjust the apparent line reactance and (ii) discussion of how the models can be efficiently integrated in operation models. In DC power flow, only the active power flow is considered. Therefore, modelling in this section is solely focused on transmission line reactance adjustment, as well as changes in active power flow caused by FACTS.

2.1. Injection modelling of FACTS compensation

In this section the derivations are based on b-θ power flow equation. However, due to its superior computational performance, all industry implementations of operation and planning problems use the ISF formulation [13]. The ISF for a transmission line represents the fraction of power injection at a certain bus that flows through this line. Using an ISF formulation eliminates the need for calculating bus voltage angles, thus, improving the scalability of DC-based models with respect to network size, compared to the b - θ formulation (1) [13]. This is the main reason that ISF-based models are widely used in industry practices. Thus, in order to enable smooth integration with existing energy and market management systems, this paper includes an injection model for each FACTS device, where the compensation is modelled as an injection pair at the two ends of the line, on which the FACTS device is installed [15]. The injection model, shown in Fig. 1, preserves the offline calculated ISF matrix of the system even with FACTS deployment, and enhances computational tractability.

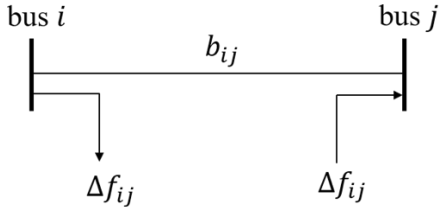

Fig. 1. *Nodal injection model of FACTS*

For the transmission line in Fig. 1, the DC power flow equation is formulated as follows:

$$f_{ij} = \left(b_{ij} + \Delta b_{ij}\right)(\theta_j - \theta_i). \quad (3)$$

(3) can be further derived to:

$$f_{ij} = b_{ij}(\theta_j - \theta_i) + \Delta b_{ij}(\theta_j - \theta_i) = \tilde{f}_{ij} + \Delta f_{ij}, \quad (4)$$

where

$$\tilde{f}_{ij} = b_{ij}(\theta_j - \theta_i), \quad (5)$$

$$\Delta f_{ij} = \Delta b_{ij}(\theta_j - \theta_i). \quad (6)$$

In (5), $\tilde{f}_{ij}$ only has the original susceptance of the line, allowing it to be calculated using the ISFs. The calculation is presented in Section 3 in the problem formulations. The impact of reactance injection is separated from the original line susceptance. The impact of FACTS adjustment, thus, can be modelled as injections, which is Δf_{ij}, at end buses of a transmission line [13].

2.2. SSSC and M-SSSC

The SSSC is one of the most important FACTS devices for transmission line series compensation [27] and has been used as one of the M-FACTS devices in the industry. The SmartValve™ [28] by Smart Wires Inc. is an M-SSSC that provides the functionality of a series capacitor or series reactor. The configuration of the SSSC is presented in Fig. 2, where the device consists of an inverter, a capacitor, and a coupling transformer. The SSSC is series connected with a transmission line through the coupling transformer [29].

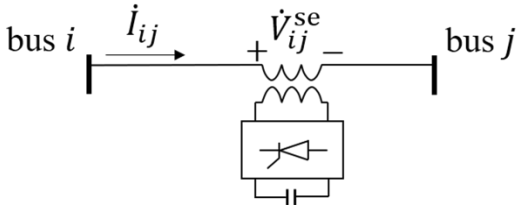

Fig. 2. *SSSC configuration [29]*

Line reactance adjustment is achieved through a series injected voltage that is in quadrature with and independent of the line current. For line ij with the SSSC installed, the quadrature phase is defined as follows [29]:

$$\mathrm{Re}\{\dot{V}_{ij}^{se}\dot{I}_{ij}^{*}\} = 0. \quad (7)$$

The magnitude of the voltage injection is constrained by its upper bound $V_{ij}^{\max}$. The operating range of voltage injection and effective reactance of the SSSC is shown in Fig. 3. Note that the device requires a minimum line current to be powered up, since it depends on the line current to power the converter through a coupling transformer. We can see that the operating range in Fig. 3 (b) is highly nonlinear.

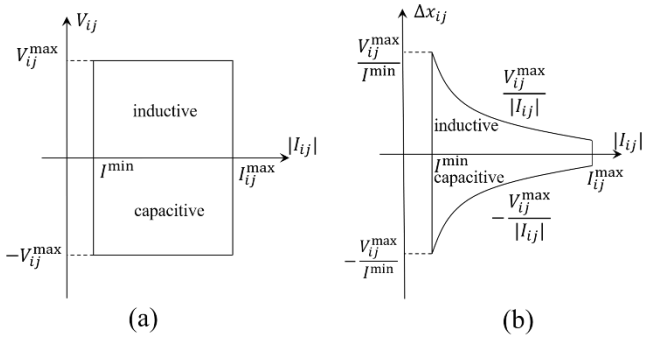

Fig. 3. *The SSSC operating range regarding: (a) voltage-current (b) reactance-current*

The effective reactance injection operating limits of SSSC devices are functions of the line current. For a transmission line, from bus i to bus j that is equipped with an SSSC, we have:

$$-V_{ij}^{\max} \le \Delta x_{ij}|I_{ij}| \le V_{ij}^{\max}. \quad (8)$$

The approximate equality between line current and active power flow in DC power flow is shown in (9) [30].

$$|I_{ij}| \approx |f_{ij}| \quad (9)$$

Using (9), while removing the absolute value sign, (8) can be reformulated as:

$$-V_{ij}^{\max} \le \Delta x_{ij} f_{ij} \le V_{ij}^{\max}. \quad (10)$$

With the effective reactance injection, we can formulate the corresponding line susceptance change as:

$$\Delta b_{ij} = -\frac{1}{x_{ij}+\Delta x_{ij}} - b_{ij}. \quad (11)$$

Solving Δx_{ij} from (11), we get:

$$\Delta x_{ij} = \frac{\Delta b_{ij}}{b_{ij}(b_{ij}+\Delta b_{ij})}. \quad (12)$$

Next, consider the DC power flow equation (3), we can further derive (12) to get:

$$\Delta x_{ij} = \frac{\Delta b_{ij}(\theta_j-\theta_i)}{b_{ij}(b_{ij}+\Delta b_{ij})(\theta_j-\theta_i)} = \frac{\Delta f_{ij}}{b_{ij} f_{ij}}. \quad (13)$$

Thus, (10) can be reformulated as:

$$-V_{ij}^{\max} \le \frac{\Delta f_{ij}}{b_{ij}} \le V_{ij}^{\max}. \quad (14)$$

Therefore, we can get the following constraints on Δf_{ij}:

$$-V_{ij}^{\max}|b_{ij}| \le \Delta f_{ij} \le V_{ij}^{\max}|b_{ij}|, \quad (15)$$

where variation limits of FACTS power injection are imposed. The limits are determined by the maximum voltage injection of the SSSC device and the original line susceptance.

Thus far, we derived (15), which is a linear constraint, from the highly nonlinear constraint in (8). The linear model allows the effective reactance injection operating range to be efficiently included in the ISF-based DC models.

As is shown in Fig. 3 (b), the variation bounds on Δx_{ij} are dependent on line current (or equivalently active power flow in DC power flow). Therefore, selecting variation limits on FACTS reactance/susceptance adjustment to apply the variable-susceptance model is nearly impossible, and the consequential inaccuracy in reflecting the power flow capabilities will be substantial. Furthermore, it is worth noting that, as mentioned previously, the variation of line susceptance in the b-θ formulation (1) makes the DCOPF problem a nonlinear program (NLP). If the variation range of line susceptance is simply modelled as in (2), assuming negative line susceptance, the constraint on FACTS nodal injection can be formulated as follows:

$$\text{For } \tilde{f}_{ij} \ge 0: \frac{(b_{ij}^{\max}-b_{ij})}{b_{ij}}\tilde{f}_{ij} \le \Delta f_{ij} \le \frac{(b_{ij}^{\min}-b_{ij})}{b_{ij}}\tilde{f}_{ij}, \quad (16)$$

$$\text{For } \tilde{f}_{ij} < 0: \frac{(b_{ij}^{\min}-b_{ij})}{b_{ij}}\tilde{f}_{ij} \le \Delta f_{ij} \le \frac{(b_{ij}^{\max}-b_{ij})}{b_{ij}}\tilde{f}_{ij}. \quad (17)$$

The corresponding nonconvex feasible region, as well as the variation limits that are defined in (15), are presented in Fig. 4.

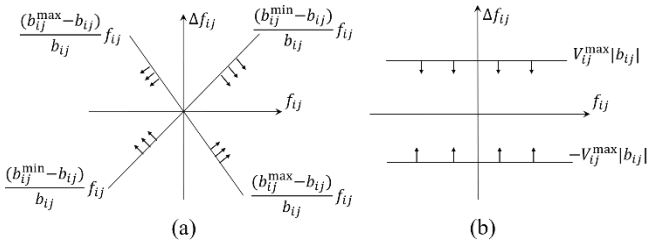

Fig. 4. *Feasible region (a) when SSSC operating range is modelled using the variable-susceptance model and (b) when considering the actual effective reactance injection operating range; arrows in the figure indicate the region defined by the corresponding constraints*

The comparison between Fig. 4 (a) and (b) reveals that the appropriate modelling of the reactance injection operating range, developed in this paper, is convex. This is contrary to the nonconvex range that is calculated in the literature [11-13], [17], [20]. Linear FACTS modelling, thus, shows substantial superiority in both accuracy and computational efficiency of the operation models for the SSSC and similar devices.

The modular nature and lightweight enclosure of M-FACTS devices allow more efficient deployment and re-deployment compared to conventional devices, providing more flexibility in installation and planning [31]. Unlike conventional FACTS devices, sizing of an M-FACTS project will determine the number of modules that are deployed at each location. Therefore, in planning problems that involves M-FACTS, integer variables should be used to model the size of the project. Thus, for M-FACTS devices that are based on the SSSC, (15) can be rewritten as:

$$-N_{ij}^{\text{FACTS}}\overline{V}\left|b_{ij}\right| \le \Delta f_{ij} \le N_{ij}^{\text{FACTS}}\overline{V}\left|b_{ij}\right|, \tag{18}$$

where an integer variable is added. (18) is, thus, a mixed-integer linear constraint. Note that (18) should be specified for planning models. In operation models, (18) is equivalent to constraint (15) as the values of N_{ij}^{FACTS} will already be determined.

2.3. MERS

The MERS is an alternative series compensator with advantages including simple configuration, low losses, low cost implementation, and zero turn-on current [32], [33]. The configuration of the MERS, which consists of a capacitor, four diodes, and four controllable switches, is shown in Fig. 5 [33].

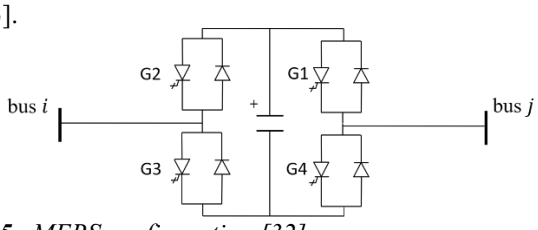

Fig. 5. *MERS configuration [32]*

The MERS provides series compensation by injecting a capacitive series voltage that lags behind the line current by 90 degrees. The size of the injected voltage can be controlled from zero to the rated voltage within the device current rating [32], [33]. Therefore, the operating range shown in Fig. 6 is the same as the capacitive voltage operating range of the SSSC [33]. For line ij with MERS devices installed, the equivalent capacitive series injection provided by the MERS is subject to the following constraints:

$$-V_{ij}^{\max} \le \Delta x_{ij}|f_{ij}| \le 0\ . \tag{19}$$

The variation limits of nodal injection of the MERS are, thus, similar to (15). However, because of the absolute value sign, they are dependent on flow direction. Combine (19) with (13), we get the following reformulated constraints.

$$\text{For } f_{ij} \ge 0\text{: } -V_{ij}^{\max} \le \frac{\Delta f_{ij}}{b_{ij}} \le 0. \tag{20}$$

$$\text{For } f_{ij} < 0\text{: } 0 \le \frac{\Delta f_{ij}}{b_{ij}} \le V_{ij}^{\max}. \tag{21}$$

The big-*M* method can used to obtain a mixed-integer linear reformulation of (20) and (21), which is presented as follows:

$$-z_{ij}M \le \frac{\Delta f_{ij}}{b_{ij}} \le V_{ij}^{\max} + z_{ij}M, \tag{22}$$

$$-V_{ij}^{\max} + \left(z_{ij}-1\right)M \le \frac{\Delta f_{ij}}{b_{ij}} \le (1-z_{ij})M, \tag{23}$$

$$\left(z_{ij}-1\right)M \le \Delta f_{ij} + \tilde{f}_{ij} \le z_{ij}M, \tag{24}$$

$$z_{ij} \in \{0,1\}, \tag{25}$$

$$M \gg \max\{f_{ij}^{\max}, V_{ij}^{\max}\}. \tag{26}$$

The binary variable, z_{ij}, is used to represent the power flow direction. The value of M can be set according to (26). The inclusion of binary variables adds more computational burden compared to (15).

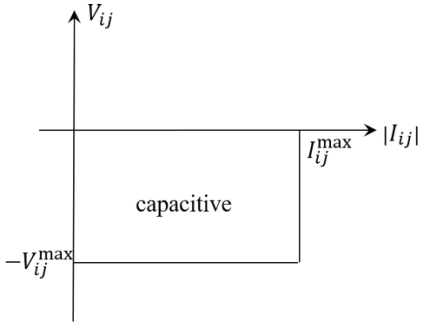

Fig. 6. *Voltage-current operating range for MERS*

2.4. UPFC

The UPFC provides real-time control and dynamic compensation of the AC transmission systems [34] and is the most versatile FACTS device [35]. The configuration of the UPFC is shown in Fig. 7 [29].

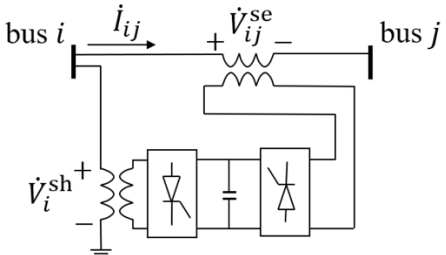

Fig. 7. *UPFC configuration [29]*

The series device of the UPFC is series connected with the transmission line through a coupling transformer. The shunt-connected transformer couples the shunt device to a local bus [29]. The series device of a UPFC can be regarded as a voltage source that is controllable in both magnitude and phase angle [36], [37]. UPFC devices provide the series compensation by regulating the series voltage injection to control the effective reactance of transmission lines [29]. Therefore, UPFC can be modelled as a controllable series voltage injection in power flow control, which is similar to the modelling of the SSSC. In addition, when comparing Fig. 7 with Fig. 2 we can see that the SSSC is the UPFC without the shunt device, which leads to the similarity in modelling.

Suppose a UPFC provides series compensation on a transmission line ij. Based on the modelling of the UPFC as a controllable voltage injection, the active power flow on the line can be formulated as:

$$f_{ij} = \mathrm{Re}\{\dot{V}_i \dot{I}_{ij}^*\} = \mathrm{Re}\left\{\frac{\dot{V}_i\left(\dot{V}_i - \dot{V}_{ij}^{\mathrm{se}} - \dot{V}_j\right)^*}{-jx_{ij}}\right\}$$
$$= \mathrm{Re}\left\{\frac{-\dot{V}_i\left(\dot{V}_j + \dot{V}_{ij}^{\mathrm{se}}\right)^*}{-jx_{ij}}\right\} \quad (27)$$

where $|\dot{V}_i| = |\dot{V}_j| = 1$ p.u., which is based on the assumptions in DC power flow [30]. (27) can, then, be formulated as:

$$f_{ij} = \mathrm{Re}\left\{\frac{-\dot{V}_i(\dot{V}_j + \dot{V}_{\mathrm{se}})^*}{-jx_{ij}}\right\}$$
$$= -\frac{1}{x_{ij}}\cos\left(\theta_i - \theta_j + \frac{\pi}{2}\right) - \frac{|\dot{V}_{\mathrm{se}}|}{X_{ij}}\cos\left(\theta_i - \varphi_{ij} + \frac{\pi}{2}\right) =$$
$$\frac{\sin(\theta_i - \theta_j)}{x_{ij}} + \frac{|\dot{V}_{\mathrm{se}}|}{x_{ij}}\sin(\theta_i - \varphi_{ij})$$
$$= b_{ij}(\theta_j - \theta_i) + |\dot{V}_{ij}^{\mathrm{se}}| b_{ij}\sin(\theta_i - \varphi_{ij}). \quad (28)$$

The FACTS power injection in the nodal injection model is, then, formulated as:

$$\Delta f_{ij} = |\dot{V}_{ij}^{\mathrm{se}}| b_{ij}\sin(\theta_i - \varphi_{ij}), \quad (29)$$

where $|\dot{V}_{ij}^{\mathrm{se}}|$ and $\sin(\theta_i - \varphi_{ij})$ satisfy the following constraints:

$$0 \le |\dot{V}_{ij}^{\mathrm{se}}| \le V_{ij}^{\max}, \quad (30)$$

$$-1 \le \sin(\theta_i - \varphi_{ij}) \le 1. \quad (31)$$

The bounds on Δf_{ij} are, thus, determined as:

$$-V_{ij}^{\max}|b_{ij}| \le \Delta f_{ij} \le V_{ij}^{\max}|b_{ij}|, \quad (32)$$

which is exactly the same as (15). Therefore, UPFC and SSSC devices show consistency in flow variation limits for FACTS power injection. The SSSC operation can be considered as a specific case for the UPFC where the injected voltage is in quadrature with the line current. In addition, UPFC devices have been viewed as combinations of the SSSC and the static synchronous compensator (STATCOM) [38]. Consider the case where UPFC injects a voltage that is in quadrature with line current, with the phase angle of:

$$\varphi_{ij} = \frac{\theta_i + \theta_j \pm \pi}{2}. \quad (33)$$

Applying this phase angle to (29), we get:

$$\Delta f_{ij} = |\dot{V}_{ij}^{\mathrm{se}}| b_{ij}\sin\left(\theta_i - \frac{\theta_i + \theta_j \pm \pi}{2}\right)$$
$$= |\dot{V}_{ij}^{\mathrm{se}}| b_{ij}(\pm\cos\left(\frac{\theta_i - \theta_j}{2}\right))$$
$$= \pm|\dot{V}_{ij}^{\mathrm{se}}| b_{ij}, \quad (34)$$

where the FACTS power injection has the same variation limits as in (15), considering the same operating range for the magnitude of the voltage injection.

2.5. TCSC

A TCSC module consists of a capacitor that is in parallel with a thyristor-controlled inductor [29], [39], [40]. The configuration of a TCSC module is shown in Fig. 8.

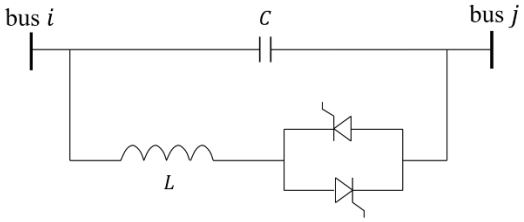

Fig. 8. *TCSC configuration [29]*

The equivalent reactance injection of a single module TCSC is, thus, controlled by the firing angle of the thyristor. The operating range is shown in Fig. 9 [41].

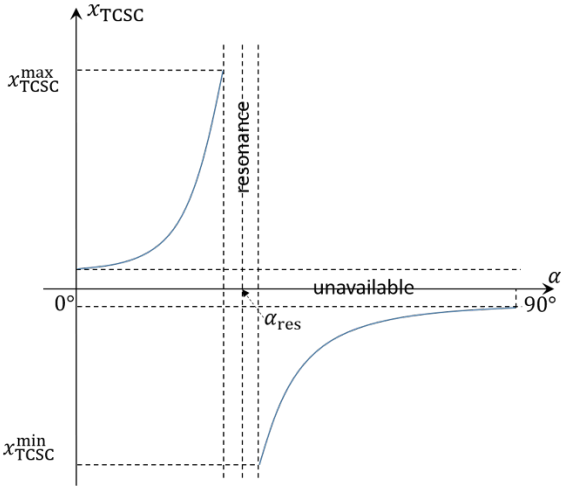

Fig. 9. *Reactance injection range of an individual module of TCSC as a function of the firing angle [41]*

In Fig. 9, α is the firing angle and α_{res} is the resonance angle. As multiple TCSC modules can be connected in series and operate independently, the unavailable band around zero reactance injection can be covered [41], allowing the TCSC to be modelled, in steady state, as a variable series reactance with continuous operating range. The static model of the TCSC is shown in Fig. 10. Note that line resistance is neglected as it is not considered in DC power flow.

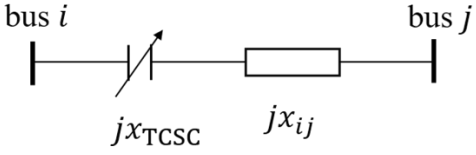

Fig. 10. *Static model of TCSC variable series reactance*

In several previous studies, the TCSC is considered to only provide capacitive reactance injection [42-44]. In this paper, we use a general model, where the TCSC can provide both inductive and capacitive series reactance compensation on transmission lines. The maximum inductive and capacitive series compensation levels of the TCSC on transmission line ij are, typically, set as follows to avoid overcompensation [45], [46]:

$$-0.8|x_{ij}| \leq \Delta x_{ij} \leq 0.2|x_{ij}|. \quad (35)$$

The variation limits of adjusted line susceptance are, thus, determined as follows:

$$b_{ij}^{\min} = -\frac{1}{x_{ij}+x_{\text{TCSC}}^{\min}}, \quad (36)$$

$$b_{ij}^{\max} = -\frac{1}{x_{ij}+x_{\text{TCSC}}^{\max}}. \quad (37)$$

The constraint on FACTS nodal power injection for TCSC is, thus, the same as (16) and (17), assuming negative line susceptance. Using the big-M method and introducing the binary variable to represent flow directions, the constraint can be reformulated as:

$$\frac{(b_{ij}^{\max}-b_{ij})}{b_{ij}} f_{ij} - z_{ij}M \leq \Delta f_{ij} \leq \frac{(b_{ij}^{\min}-b_{ij})}{b_{ij}} f_{ij} + z_{ij}M, \quad (38)$$

$$(z_{ij}-1)M + \frac{(b_{ij}^{\min}-b_{ij})}{b_{ij}} f_{ij} \leq \Delta f_{ij} \leq (1-z_{ij})M + \frac{(b_{ij}^{\max}-b_{ij})}{b_{ij}} f_{ij}, \quad (39)$$

$$-z_{ij}M \leq f_{ij} \leq \left(1-z_{ij}\right)M, \quad (40)$$

$$z_{ij} \in \{0,1\} \quad (41)$$

$$M \gg \max\left\{f_{ij}^{\max}, \frac{(b_{ij}^{\min}-b_{ij}^{\max})}{b_{ij}} f_{ij}^{\max}\right\}. \quad (42)$$

The reformulation presented in (38)-(42) is equivalent to the ones in [11-13], [20]. Note that the linearity in the reformulation allows the DCOPF and UC problems involving TCSC to be solved more efficiently than problems formulated with the original nonlinear constraints.

3. Problem formulation

In this section, we incorporate linear FACTS modelling into power system operation models DCOPF and UC. In addition, we formulate the DCOPF and UC problems with nonlinear FACTS modelling. For simplicity, we name each problem formulation according to the following format: device type_ FACTS modelling (L: linear FACTS modelling; NL: nonlinear FACTS modelling)_operation model (OPF or UC). The formulated problems are studied through simulations in Section 4. As the nonlinear power flow control equations are formulated directly from the operating ranges of FACTS devices, the results of the problems with nonlinear formulations can be used for verifying the mathematical derivation leading to linear FACTS modelling. Moreover, the solution time are compared to show the computational efficiency improvement provided by the application of linear FACTS modelling.

Note that for devices that rely on current as source of power, an extra constraint may need to be considered:

$$|\tilde{f}_{ij} + \Delta f_{ij}| \geq f^{\min}. \quad (43)$$

(43) is a not a linear constraint, which is undesirable for optimisation solvers. It can be reformulated to a mixed-integer linear constraint, using the big-M method, for which efficient solvers are available.

$$\tilde{f}_{ij} + \Delta f_{ij} + z_{ij}M \geq f^{\min} \quad (44)$$

$$\tilde{f}_{ij} + \Delta f_{ij} \leq -f^{\min} + (1-z_{ij})M \quad (45)$$

$$z_{ij} \in \{0,1\} \quad (46)$$

$$M \gg \max\{f_{ij}^{\max} + f^{\min}\} \quad (47)$$

Inclusion of (44)-(47) increases the computational complexity of power system operation models. However, power flow reaching the limits of (44) and (45) indicates that the line is very lightly utilised, which implies that it is an ineffective location for FACTS deployment in the first place. Therefore, it is unlikely for (44) and (45) to become active, if FACTS devices are allocated appropriately. The two constraints, thus, can usually be removed from the problem formulation, without affecting the solution.

For modular FACTS devices such as the M-SSSC, the number of modules deployed on each transmission line needs to be optimised as well. Therefore, the following constraints needs to be included in the problem formulation, along with (18):

$$N_{ij}^{\text{FACTS}} \leq N_{ij}^{\max}, \quad (48)$$

$$\sum_{i,j} N_{ij}^{\text{FACTS}} \leq N^{\max}. \quad (49)$$

(48) is the constraint on the maximum number of devices allowed to be deployed on transmission line ij. Note that this limit is line specific and depends on a number of factors, such as physical size and weight of M-FACTS, distance between transmission towers, etc. (49) specifies the availability constraint of M-SSSC devices.

3.1. Problem formulation with linear FACTS modelling

We first present the objective function and the constraints that are common for ISF-based DCOPF [13] with FACTS regardless of the choice of FACTS device type. The DCOPF problem without the power flow control constraints can be partially formulated as follows:

$$\text{minimise} \sum_{g\in G} c_g p_g \quad (50)$$

s.t.

$$f_{ij} = \sum_{n\in N} \Phi_{ij}^{n} \psi_n, \forall ij \notin K_{\text{F}}; \quad (51)$$

$$\tilde{f}_{ij} = \sum_{n\in N} \Phi_{ij}^{n} \psi_n, \forall ij \in K_{\text{F}}; \quad (52)$$

$$\psi_i = \sum_{g\in G(i)} p_g - d_i + \sum_{j\in N^+(i)} \Delta f_{ij} - \sum_{j\in N^-(i)} \Delta f_{ij}, \forall i; \quad (53)$$

$$p_g^{\min} \leq p_g \leq p_g^{\max}, \forall g; \quad (54)$$

$$\sum_{g\in G} p_g = \sum_{i\in N} d_i, \forall g, i; \quad (55)$$

$$-f_{ij}^{\max} \leq f_{ij} \leq f_{ij}^{\max}, \forall ij \notin K_{\text{F}}; \quad (56)$$

$$-f_{ij}^{\max} \leq \tilde{f}_{ij} + \Delta f_{ij} \leq f_{ij}^{\max}, \forall ij \in K_{\text{F}}. \quad (57)$$

(50) is the objective function where the total generation cost is minimised, assuming linear marginal costs for generators. Power flows are calculated using ISFs in (51) and (52). Note that in (52), only the power flow without

FACTS injection is calculated for lines with FACTS devices installed. In (53), power injection at each bus is calculated using generation, demand, and FACTS nodal injection. The generator operating capacities are specified in (54). (55) represents the power balance in the network. Thermal capacity limits of transmission lines are presented in (56) and (57).

We then need the power flow control constraints to formulate the full DCOPF problems. These constraints have been formulated in the mathematical derivations in Section 2. For each specific DCOPF problem formulation, the power flow control constraints are listed as follows:

SSSC_L_OPF & UPFC_L_OPF:
(15).

MERS_L_OPF:
(22)-(26).

TCSC_L_OPF:
(38)-(42).

M-SSSC_L_OPF:
(18), (48)-(49).

Linear FACTS modelling preserves the desirable characteristic of linearity of the original DCOPF problem. Both SSSC_L_OPF and UPFC_L_OPF are linear programs (LP) because (15) is a linear constraint. The other three formulations are mixed-integer linear programs (MILP) due to the presence of integer variables. The DCOPF formulations can be extended to other operation and planning applications, for instance, security-constrained optimal power flow (SCOPF).

The linear power flow control constrains can be utilised in ISF-based UC problems as well. Similarly, ISF-based UC problems can first be partially formulated as follows:

$$\text{minimise} \sum_{g\in G}\sum_{t\in T}(c_g p_{gt} + k_g u_{gt} + s_g v_{gt}) \quad (58)$$

s.t.

$$f_{ij,t} = \sum_{n\in N} \Phi_{ij}^{n} \psi_{nt}, \forall ij \notin K_{\mathrm{F}}, t; \quad (59)$$

$$\tilde{f}_{ij,t} = \sum_{n\in N} \Phi_{ij}^{n} \psi_{nt}, \forall ij \in K_{\mathrm{F}}, t; \quad (60)$$

$$\psi_{it} = \sum_{g\in G(i)} p_{gt} - d_{it} + \sum_{j\in N^{+}(i)} \Delta f_{ij,t} - \sum_{j\in N^{-}(i)} \Delta f_{ij,t}, \forall i, t; \quad (61)$$

$$u_{gt} p_{gt}^{\min} \le p_{gt} \le u_{gt} p_{gt}^{\max}, \forall g, t; \quad (62)$$

$$\sum_{g\in G} p_{gt} = \sum_{i\in N} d_{it}, \forall t; \quad (63)$$

$$-f_{ij}^{\max} \le f_{ij,t} \le f_{ij}^{\max}, \forall ij \notin K_{\mathrm{F}}, t; \quad (64)$$

$$-f_{ij}^{\max} \le \tilde{f}_{ij,t} + \Delta f_{ij,t} \le f_{ij}^{\max}, \forall ij \in K_{\mathrm{F}}, t; \quad (65)$$

$$-R_g^{-} \le p_{gt} - p_{g,t-1} \le R_g^{+}, \forall g, t; \quad (66)$$

$$\sum_{r=t-UT_g+1}^{t} v_{gr} \le u_{gr}, \forall g, t \ge UT_g; \quad (67)$$

$$\sum_{r=t+1}^{t+DT_g} v_{gr} \le 1 - u_{gr}, \forall g, t \le |T| - DT_g; \quad (68)$$

$$u_{gt} - u_{g,t-1} \le v_{gt}, \forall g, t; \quad (69)$$

$$u_{gt} \in \{0, 1\}, \forall g, t; \quad (70)$$

$$0 \le v_{gt} \le 1, \forall g, t. \quad (71)$$

As is shown in (58), the objective of the UC problem is to minimise the summation of production cost, start-up cost, and no-load cost of the generators [47]. (59)-(65) are interpreted similarly to (51)-(57), with differences being the added time index and binary commitment variables in (62). (66) specifies the ramping constraints of generators. Minimum up and down time constraints are represented by (67)-(68) [48]. (69) represents the relationship between commitment variables and start-up variables. (70) specifies that commitment variables are binary. (71) defines the upper and lower bounds of start-up variables. Note that start-up variables can be relaxed from being binary to being continuous as they will be forced to the extremes in the UC solutions.

Again, the power flow control constraints are needed to complete the UC problem formulations. Power flow control constraints with linear FACTS modelling for each specific problem formulation are presented as follows:

SSSC_L_UC & UPFC_L_UC:

$$-V_{ij}^{\max}\left|b_{ij}\right| \le \Delta f_{ij,t} \le V_{ij}^{\max}\left|b_{ij}\right|, \forall ij \in K_{\mathrm{F}}; \quad (72)$$

MERS_L_UC:
(26),

$$-z_{ij,t}M \le \frac{\Delta f_{ij,t}}{b_{ij}} \le V_{ij}^{\max} + z_{ij,t}M, \forall ij \in K_{\mathrm{F}}; \quad (73)$$

$$-V_{ij}^{\max} + \left(z_{ij,t} - 1\right)M \le \frac{\Delta f_{ij,t}}{b_{ij}} \le \left(1 - z_{ij,t}\right)M, \forall ij \in K_{\mathrm{F}}; \quad (74)$$

$$\left(z_{ij,t} - 1\right)M \le \Delta f_{ij,t} + \tilde{f}_{ij,t} \le z_{ij,t}M, \forall ij \in K_{\mathrm{F}}; \quad (75)$$

$$z_{ij,t} \in \{0, 1\}, \forall ij \in K_{\mathrm{F}}; \quad (76)$$

TCSC_L_UC:
(42), (76),

$$\frac{(b_{ij}^{\max} - b_{ij})}{b_{ij}} f_{ij,t} - z_{ij,t}M \le \Delta f_{ij,t} \le \frac{(b_{ij}^{\min} - b_{ij})}{b_{ij}} f_{ij,t} + z_{ij,t}M, \forall ij \in K_{\mathrm{F}}; \quad (77)$$

$$(z_{ij} - 1)M + \frac{(b_{ij}^{\min} - b_{ij})}{B_{ij}} f_{ij,t} \le \Delta f_{ij,t} \le (1 - z_{ij})M + \frac{(b_{ij}^{\max} - b_{ij})}{B_{ij}} f_{ij,t}, \forall ij \in K_{\mathrm{F}}; \quad (78)$$

$$-z_{ij,t}M \le f_{ij,t} \le \left(1 - z_{ij,t}\right)M, \forall ij \in K_{\mathrm{F}}; \quad (79)$$

M-SSSC_L_UC:
(48)-(49),

$$-N_{ij}^{\mathrm{FACTS}}\overline{V}\left|b_{ij}\right| \le \Delta f_{ij,t} \le N_{ij}^{\mathrm{FACTS}}\overline{V}\left|b_{ij}\right|, \forall ij \in K_{\mathrm{F}}. \quad (80)$$

The complete problems are then formulated by selecting the power flow control constraints based on the device type. As each of the formulations involves linear FACTS modelling as well as integer variables, all the problems are MILPs. We can expand the UC formulations to a variety of other more complicated models as well, including security-constrained unit commitment (SCUC) and stochastic unit commitment (SUC).

3.2. Problem formulation with nonlinear FACTS modelling

The formulated problems, as mentioned previously, are solved in simulations for verification and exploring computational efficiency gains provided by linear FACTS modelling. Therefore, we need to formulate the DCOPF and UC problems using the nonlinear power flow control constraints as well. For these formulations, we use the original DCOPF formulations without shift factors because of the direct modelling of FACTS compensation in nonlinear power flow control constraints. Following a similar approach, we first present the partial formulation of DCOPF without power flow control constraints.

The objective function is, still, (50), and the operating capacity constraints for generators are specified in (54). The rest of the constraints, except for the power flow control constraints, are presented as follows:

$$-f_{ij}^{\max} \le f_{ij} \le f_{ij}^{\max}, \forall ij; \quad (81)$$

$$\sum_{g\in G(i)} p_g + \sum_{j\in N^+(i)} f_{ij} - \sum_{j\in N^-(i)} f_{ij} = d_i, \forall i; \quad (82)$$

$$f_{ij} = -\frac{\theta_j-\theta_i}{x_{ij}}, \forall ij \notin K_{\mathrm{F}}; \quad (83)$$

$$\theta_1 = 0. \quad (84)$$

(81) imposes the thermal capacity limits on transmission line ij. (82) is the power balance constraint at bus i. (83) is the DC power flow equation for lines without FACTS. (84) ensures that the voltage angle at the reference bus is equal to zero.

The power flow control constraints with nonlinear FACTS modelling, along with the partial formulation discussed previously, are used to formulated complete DCOPF problems. The power flow control constraints involving each type of FACTS devices for DCOPF problems are presented as follows:

SSSC_NL_OPF:
(10),

$$f_{ij} = -\frac{\theta_j-\theta_i}{x_{ij}+\Delta x_{ij}}, \forall ij \in K_{\mathrm{F}}; \quad (85)$$

MERS_NL_OPF:
(10), (85),

$$\Delta x_{ij} \le 0, \forall ij \in K_{\mathrm{F}}; \quad (86)$$

UPFC_NL_OPF:
(30)-(31),

$$f_{ij} = \frac{\theta_i-\theta_j}{x_{ij}} - \frac{\left|\dot{V}_{ij}^{\mathrm{se}}\right|}{x_{ij}}\sin\left(\theta_i-\varphi_{ij}\right), \forall ij \in K_{\mathrm{F}}; \quad (87)$$

TCSC_NL_OPF:
(35), (85).

M-SSSC_NL_OPF:
(48)-(49), (85),

$$-N_{ij}^{\mathrm{FACTS}}\overline{V} \le \Delta x_{ij} f_{ij} \le N_{ij}^{\mathrm{FACTS}}\overline{V}, \forall ij \in K_{\mathrm{F}}. \quad (88)$$

Compared to (80), (85) has Δx_{ij} to represent the reactance injection by FACTS devices. The combination of (10) and (85) is equivalent to (19), thus allowing a more efficient formulation for the solver to compute with the removal of the absolute sign. In (87), as φ_{ij} is a free variable, we can simply regard $\sin\left(\theta_i-\varphi_{ij}\right)$ as a continuous variable with limits being 1 and -1 when implementing the problem involving UPFC in the solver. $\left|\dot{V}_{ij}^{\mathrm{se}}\right|$ is regarded as a continuous variable as well, with variation limits specified in (30). In (88), the inclusion of N_{ij}^{FACTS} shows that the voltage injection limits are dependent on the number of modules installed on the transmission line, which is different from that in (10).

Nonlinearity in the constraints makes the DCOPF problems with nonlinear FACTS modelling NLPs except for M-SSSC_NL_OPF, which is a mixed-integer nonlinear program (MINLP) as it contains integer variables.

We then formulate the UC problems with nonlinear FACTS modelling, starting with the partial formulation. The objective function is (58). Constraints (62)-(71) are the same as in the UC problems with linear FACTS modelling. The rest of the constraints, except for the power flow control constraints, are formulated as follows:

$$-f_{ij,t}^{\max} \le f_{ij,t} \le f_{ij,t}^{\max}, \forall ij, t; \quad (89)$$

$$\sum_{g\in G(i)} p_{gt} + \sum_{j\in N^+(i)} f_{ij,t} - \sum_{j\in N^-(i)} f_{ij,t} = d_{it}, \forall i, t; \quad (90)$$

$$f_{ij,t} = -\frac{\theta_{jt}-\theta_{it}}{x_{ij}}, \forall ij \notin K_{\mathrm{F}}, t; \quad (91)$$

$$\theta_{1t} = 0, \forall t. \quad (92)$$

The interpretation of (89)-(92) is the same as that of (81)-(84), except for the added time index.

Nonlinear power flow control constraints are needed to complete the UC problem formulations. These constraints can be formulated by simply adding the time index to the previously formulated constraints. Nonlinear power flow control constraints for each specific UC problem formulation are presented as follows:

SSSC_NL_UC:

$$-V_{ij,t}^{\max} \le \Delta x_{ij,t} f_{ij,t} \le V_{ij,t}^{\max}, \forall ij \in K_{\mathrm{F}}, t; \quad (93)$$

$$f_{ij,t} = -\frac{\theta_{jt}-\theta_{it}}{x_{ij}+\Delta x_{ij,t}}, \forall ij \in K_{\mathrm{F}}, t; \quad (94)$$

MERS_NL_UC:
(93), (94),

$$\Delta x_{ij,t} \le 0, \forall ij \in K_{\mathrm{F}}, t; \quad (95)$$

UPFC_NL_UC:

$$0 \le \left|\dot{V}_{ij,t}^{\mathrm{se}}\right| \le V_{ij}^{\max}, \forall ij \in K_{\mathrm{F}}, t; \quad (96)$$

$$-1 \le \sin\left(\theta_{it}-\varphi_{ij,t}\right) \le 1, \forall ij \in K_{\mathrm{F}}, t; \quad (97)$$

$$f_{ij} = \frac{\theta_{it}-\theta_{jt}}{x_{ij}} + \frac{\left|\dot{V}_{ij,t}^{\mathrm{se}}\right|}{x_{ij}}\sin\left(\theta_{it}-\varphi_{ij,t}\right), \forall ij \in K_{\mathrm{F}}, t; \quad (98)$$

TCSC_NL_UC:
(94),

$$-0.8|x_{ij}| \le \Delta x_{ij,t} \le 0.2|x_{ij}|, \forall ij \in K_{\mathrm{F}}, t; \quad (99)$$

M-SSSC_NL_UC:
(48)-(49), (94),

$$-N_{ij}^{\mathrm{FACTS}}\overline{V} \le \Delta x_{ij,t} f_{ij,t} \le N_{ij}^{\mathrm{FACTS}}\overline{V}, \forall ij \in K_{\mathrm{F}}, t. \quad (100)$$

$\left|\dot{V}_{ij,t}^{\mathrm{se}}\right|$ and $\sin\left(\theta_{it}-\varphi_{ij,t}\right)$ are regarded as continuous variables when the problems involving UPFC is implemented in the solver. Because of the nonlinear constraints and integer

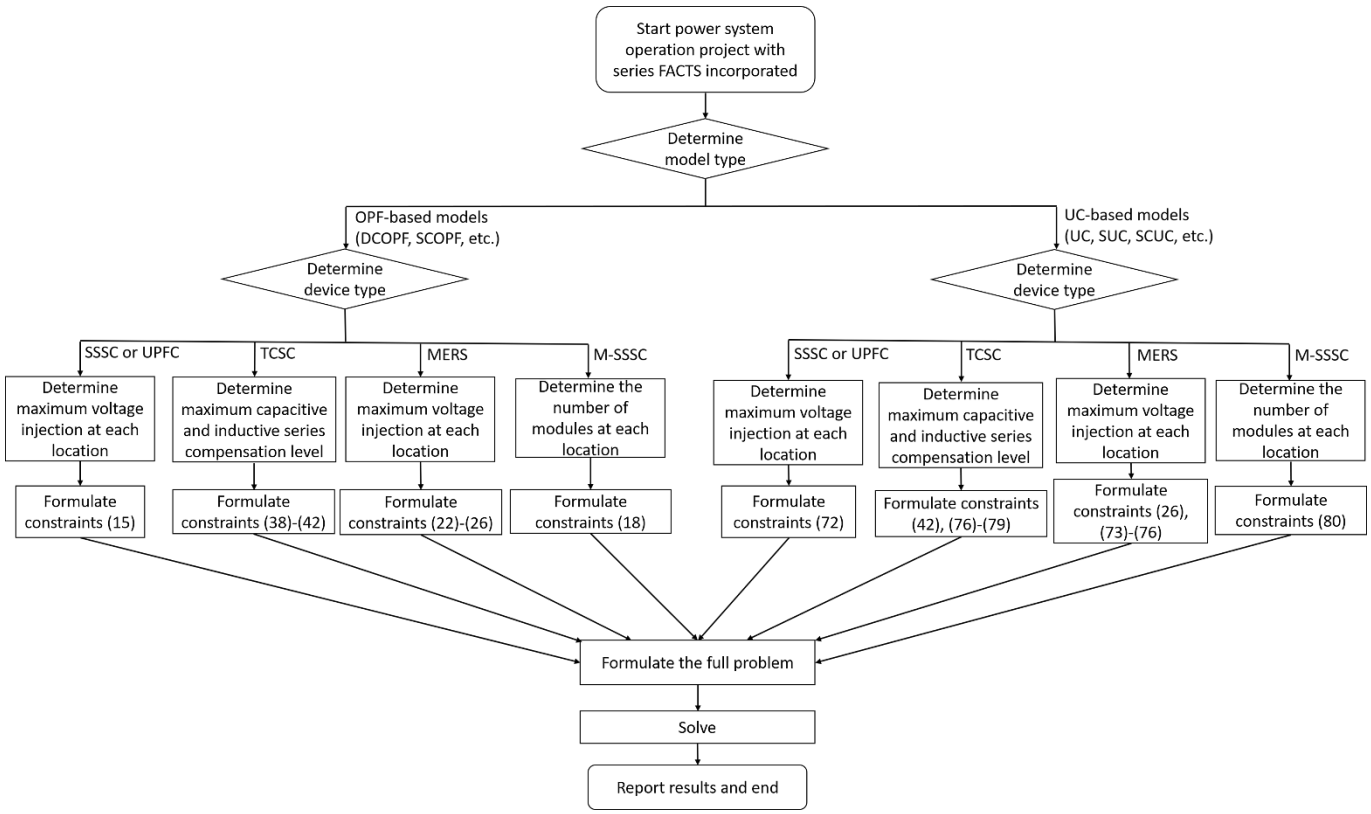

Fig. 11. *Incorporation of series FACTS into power system operation using linear FACTS models*

variables, all UC problems with nonlinear FACTS modelling are MINLPs.

3.3. Incorporation of series FACTS into power system operation models using linear FACTS modelling

With the problem formulations using linear FACTS modelling, we can now summarise how series FACTS can be incorporated into DC-based operation models. Note that, as mentioned previously, the DCOPF and UC problem formulations can be further extended to more complicated models. The process of incorporating series FACTS devices into power system operation models using linear FACTS models is presented in Fig. 11.

4. Simulation studies

Simulation studies are conducted to evaluate the effectiveness of the proposed modelling in improving computational efficiency. At the same time, the simulation results provide numerical verification for the mathematical derivations in Section 2. For the problems formulated in the previous section, we select prominent solvers that are well-suited for their problem types. Our solver selection is summarised in Table 1.

Table 1 Solver selection in simulation studies

Problem type	Solver
LP	IBM ILOG CPLEX Studio 12.8 [49]
MILP	
NLP	IPOPT 3.11.1 [50]
MINLP	BARON 20.4.14 [51]

For MILPs and MINLPs, the optimality gap for both CPLEX and BARON solvers are set as 0.01%. Details of these parameters can be found in [52], [53]. Simulations are performed on a Windows Server with an Intel Xeon Gold 6136 CPU. The Texas 2000-bus system (ACTIVSg2000) [54] is used for DCOPF problems. The data for the test system is available at [55]. For UC problems, we use a smaller system, as the computational burden of UC plus the complexity of FACTS devices may lead to computational intractability with a large system. The system we use for UC is area 1 of the RTS-96 system [56], which is equivalent to a 24-bus test system. The test systems are modified to increase congestions, allowing them to be more suitable for studying operation models with FACTS included. The modifications are presented in the Appendix.

In the 2000-bus system, the ten lines are utilised the most are selected as locations for FACTS deployment. In the RTS-96 system, FACTS devices are deployed on each of the five lines with the largest reactance in the system, thus allowing diversity in FACTS allocation policy in the simulation studies. Note that optimal FACTS allocation is beyond the scope of this work. However, it is a key topic to be further studied in future work with the proposed modelling approach.

The sizing of FACTS at each location also needs to be specified. For the SSSC, we consider that each location has three SmartValve 10-3600 [57] devices installed, providing a maximum nominal voltage injection of 12006.67 V (0.087 p.u. for the RTS-96 system and 0.104 p.u. for the 2000-bus system). This value is used as the maximum voltage injection for MERS and UPFC devices as well. The maximum voltage injection for these three types of devices can be altered depending on the different need for power flow control capabilities in various scenarios. The setting for TCSC

devices is the same as in (35), which, as mentioned previously, is a typical setting for TCSC operating range of series reactance adjustment.

Note that problem formulations involving M-SSSC has nonbinary integer variables, making them computationally more demanding than other mixed-integer programs (MIP) in this paper. In addition, as mentioned previously, they are planning models, which is beyond the main focus of this paper which are operation models. Therefore, these problems are not studied through simulations in this paper and will be further explored in future research.

4.1. DCOPF

The results of DCOPF problems with linear FACTS modelling are summarised in Table 2. Each problem is solved for 5 times and the results are used to obtain the average and standard deviation of solution time. The SSSC and the UPFC share the same linear modelling, thus their related problem formulations share the same results in Table 2.

Table 2 Solutions and computational results of DCOPF with linear FACTS modelling

DCOPF	Obj. value (cost) ($)	Solution time avg. (s)	Solution time std. (s)
SSSC_L_OPF	882782	2.508	0.164
UPFC_L_OPF			
MERS_L_OPF	887295	1.826	0.140
TCSC_L_OPF	886134	1.722	0.122

The results of DCOPF problems with nonlinear formulations are presented in Table 3.

Table 3 Solutions and computational results of DCOPF with nonlinear FACTS modelling

DCOPF	Obj. value (cost) ($)	Solution time avg. (s)	Solution time std. (s)
SSSC_NL_OPF	882782	4.423	0.193
UPFC_NL_OPF	882782	3.681	0.143
MERS_NL_OPF	887295	2.829	0.132
TCSC_NL_OPF	886134	3.070	0.151

By comparing the objective function value results in Table 2 and Table 3, we can see that both the linear and nonlinear formulations result in the same optima for every type of FACTS device discussed in this paper. The results, thus, provide a numerical verification the mathematical derivation leading to linear FACTS modelling.

We use the average solution time as the measurement for computational efficiency. Table 4 presents the comparison regarding computational efficiency between linear and nonlinear FACTS modelling for DCOPF problems.

Table 4 Computational efficiency gain provided by linear FACTS modelling in DCOPF problems

FACTS device	Comp. efficiency gain
SSSC	176 %
MERS	155 %
UPFC	147 %
TCSC	178 %

The results reveal that linear FACTS modelling provides computational efficiency gains for DCOPF models involving different types of FACTS devices. It is worth noting that DCOPF problems are inherently less computationally challenging and, thus, we expect more computational efficiency improvement from linear FACTS modelling in more complicated models. Computational efficiency improvement is further discussed with the results of UC problems, which are presented in the next subsection.

4.2. UC

The results of UC problems with linear FACTS modelling are summarised in Table 5. Table 6 presents the results of UC problems with nonlinear formulations.

Table 5 Solutions and computational results of UC with linear FACTS modelling

UC	Obj. value (cost) ($)	Solution time avg. (s)	Solution time std. (s)
SSSC_L_UC	973049	1.044	0.087
UPFC_L_UC			
MERS_L_UC	973170	1.100	0.066
TCSC_L_UC	973464	16.858	0.549

Table 6 Solutions and computational results of UC with nonlinear FACTS modelling

UC	Obj. value (cost) ($)	Solution time avg. (s)	Solution time std. (s)
SSSC_NL_UC	973049	141.328	17.525
UPFC_NL_UC	973049	123.916	6.553
MERS_NL_UC	973170	615.432	52.830
TCSC_NL_UC	Failed to converge after 100000 seconds		

As is shown in Table 6, the solver failed to provide a solution for TCSC_NL_UC after the maximum time limit of 100,000 seconds. This emphasises the importance of linear FACTS modelling as the nonconvexity and nonlinearity of nonlinear TCSC modelling leads to computational intractability for the basic UC problem implemented with a small test system. For the intuitiveness and explicitness of the results, we implemented TCSC_NL_UC and TCSC_L_UC with the smaller IEEE 14-bus test system [58]. The system data for the simulation studies is available in [59], and line thermal capacity data is obtained from [60]. Five lines with the largest reactance are selected as locations for FACTS deployment in the system. Again, we made modifications to the system to increase the congestion. The modifications are presented in the Appendix. The results are shown in Table 7.

Table 7 Solutions and computational results of UC with TCSC using the 14-bus system

UC	Obj. value	Solution	Solution

	(cost) ($)	time avg. (s)	time std. (s)
TCSC_ NL_UC	187092	32.670	0.989
TCSC_L_UC	187092	0.620	0.040

The objective function value results in Tables 5-7 confirmed that both the linear and nonlinear FACTS modelling achieve the same optima for UC models across all types of FACTS devices studied in this paper. The UC results, thus, provide verification for linear FACTS modelling as well.

We again use the average solution time as the measurement for computational efficiency. Table 8 presents the comparison regarding computational efficiency between linear and nonlinear FACTS modelling.

Table 8 Computational efficiency gain provided by linear FACTS modelling in UC problems

FACTS device	Comp. efficiency gain
SSSC	13537 %
MERS	55948 %
UPFC	11869 %
TCSC	5269 %

The results in Table 8 show that the linear FACTS modelling provides significant computational efficiency improvement over nonlinear FACTS modelling in UC problems. Note that for UC problems involving the TCSC, the result in Table 8 is calculated using the results presented in Table 7. The computational efficiency gain is, thus, expected to be even more significant with a larger system.

The results of UC problems reveal that linear FACTS modelling will be valuable for a variety of related power system optimisation models, including previously mentioned SCUC and SUC, as well as planning models. These models inherently bear significant computationally burdens even without FACTS deployment. Therefore, linear FACTS modelling will be important for ensuring computational tractability for complex power system optimisation models involving FACTS deployment.

5. Conclusions

This paper presents the linear modelling of series FACTS devices in power system operation models. Compared to the existing literature, the models presented here accurately captures the operating range of FACTS devices. In addition, this paper enables integration of FACTS devices within linear DC power flow models through derivation of an equivalent linear operating range. Finally, the paper shows how the constraints can be applied in injection-shift-factor-based DCOPF and UC, which are widely used in industry implementations of operation and planning software tools.

Simulation results verifies the mathematical derivation that leads to the proposed modelling. Moreover, linear FACTS modelling shows significant superiority in computational efficiency. The results underline the importance of linear FACTS modelling in combating the challenge of increased computational complexity due to FACTS deployment in the already computationally heavy optimisation models. Furthermore, linear FACTS modelling will be vital in facilitating FACTS technology deployment in the power gird. Linear FACTS modelling will be important for incorporating series FACTS into various operation and planning models, including SUC, SCOPF, and SCUC, allowing the utilization of power flow control capabilities of FACTS devices. The models presented in this paper is also vital for developing FACTS planning tools for optimal placement that are based on DC power flow models. Moreover, M-FACTS deployment problems, including optimal allocation, reinstallation scheduling, etc., will be important topics as well. Studying these problems and models will be included in our future research.

6. Acknowledgements

This research was funded by the National Science Foundation grant # 1756006.

7. References

[1] Joskow, P.L.: 'Creating a Smarter U.S. Electricity Grid'*Journal of Economic Perspectives*, 2012, **26**, (1), pp. 29–48.

[2] Sahraei-Ardakani, M.: 'Merchant power flow controllers'*Energy Economics*, 2018, **74**, pp. 878–885.

[3] Ou, Y., Singh, C.: 'Assessment of available transfer capability and margins'*IEEE Trans. Power Syst.*, 2002, **17**, (2), pp. 463–468.

[4] Del Rosso, A.D., Eckroad, S.W.: 'Energy Storage for Relief of Transmission Congestion'*IEEE Trans. Smart Grid*, 2014, **5**, (2), pp. 1138–1146.

[5] Energy Information Administration: 'Annual Energy Outlook 2021' (2021). Available at https://www.eia.gov/outlooks/aeo/

[6] Zhang, X., Shi, D., Wang, Z., *et al.*: 'Optimal Allocation of Series FACTS Devices Under High Penetration of Wind Power Within a Market Environment'*IEEE Transactions on Power Systems*, 2018, **33**, (6), pp. 6206–6217.

[7] Lumbreras, S., Ramos, A.: 'The new challenges to transmission expansion planning. Survey of recent practice and literature review'*Electric Power Systems Research*, 2016, **134**, pp. 19–29.

[8] Marston, T.U.: 'The US Electric Power System Infrastructure and Its Vulnerabilities'*The Bridge*, 2018, **48**, (2), pp. 31–39.

[9] National Energy Technology Laboratory, 'Understanding the Benefits of the Smart Grid' (2010), pp. 1-33. Available at https://netl.doe.gov/sites/default/files/Smartgrid/06-18-2010_Understanding-Smart-Grid-Benefits.pdf

[10] Sang, Y., Sahraei-Ardakani, M., Parvania, M.: 'Stochastic Transmission Impedance Control for Enhanced Wind Energy Integration'*IEEE Transactions on Sustainable Energy*, 2018, **9**, (3), pp. 1108–1117.

[11] Sahraei-Ardakani, M., Hedman, K.W.: 'A fast LP approach for enhanced utilization of variable impedance based FACTS devices'*IEEE Transactions on Power Systems*, 2016, **31**, (3), pp. 2204–2213.

[12] Sahraei-Ardakani, M., Hedman, K.W.: 'Day-Ahead Corrective Adjustment of FACTS Reactance: A Linear Programming Approach'*IEEE Transactions on Power Systems*, 2016, **31**, (4), pp. 2867–2875.

[13] Sahraei-Ardakani, M., Hedman, K.W.: 'Computationally Efficient Adjustment of FACTS Set Points in DC Optimal Power Flow With Shift Factor Structure'*IEEE Transactions on Power Systems*, 2017, **32**, (3), pp. 1733–1740.

[14] Geng, G., Abhyankar, S., Wang, X., Dinavahi, V., IEEE PES Task Force on Interfacing Techniques for Solution Tools: 'Solution techniques for transient stability-constrained optimal power flow – Part II'*IET gener. transm. distrib.*, 2017, **11**, (12), pp. 3186–3193.

[15] Yang, Z., Zhong, H., Bose, A., Zheng, T., Xia, Q., Kang, C.: 'A Linearized OPF Model With Reactive Power and Voltage Magnitude: A Pathway to Improve the MW-Only DC OPF'*IEEE Transactions on Power Systems*, 2018, **33**, (2), pp. 1734–1745.

[16] Stott, B., Jardim, J., Alsac, O.: 'DC Power Flow Revisited'*IEEE Transactions on Power Systems*, 2009, **24**, (3), pp. 1290–1300.

[17] Taranto, G.N., Pinto, L.M.V.G., Pereira, M.V.F.: 'Representation of FACTS devices in power system economic dispatch'*IEEE Trans. Power Syst.*, 1992, **7**, (2), pp. 572–576.

[18] Sahraei-Ardakani, M., Sang, Y.: 'Discussion on Linear Modeling of Variable Reactance in "Co-Optimization of Transmission Expansion Planning and TCSC Placement Considering the Correlation Between

Wind and Demand Scenarios"'*IEEE Trans. Power Syst.*, 2018, **33**, (5), pp. 5808–5809.
[19] Ziaee, O., Alizadeh-Mousavi, O., Choobineh, F.F.: 'Co-Optimization of Transmission Expansion Planning and TCSC Placement Considering the Correlation Between Wind and Demand Scenarios'*IEEE Trans. Power Syst.*, 2018, **33**, (1), pp. 206–215.
[20] Ding, T., Bo, R., Li, F., Sun, H.: 'Optimal Power Flow With the Consideration of Flexible Transmission Line Impedance'*IEEE Transactions on Power Systems*, 2016, **31**, (2), pp. 1655–1656.
[21] Mohammadi, J., Hug, G., Kar, S.: 'Fully distributed DC-OPF approach for power flow control', Proc. 2015 IEEE Power & Energy Society General Meeting, Denver, Colorado, USA, July 2015, pp. 1–5
[22] Li, B., Xiao, G., Lu, R., Deng, R., Bao, H.: 'On Feasibility and Limitations of Detecting False Data Injection Attacks on Power Grid State Estimation Using D-FACTS Devices'*IEEE Trans. Ind. Inf.*, 2020, **16**, (2), pp. 854–864.
[23] Liu, B., Wu, H.: 'Systematic planning of moving target defence for maximising detection effectiveness against false data injection attacks in smart grid'*IET cyber-phys. syst.*, 2021, p. cps2.12012.
[24] Yan, M., Shahidehpour, M., Paaso, A., Zhang, C., Abdulwhab, A., Abusorrah, A.: 'A Convex Three-Stage SCOPF Approach to Power System Flexibility with Unified Power Flow Controllers'*IEEE Trans. Power Syst.*, 2020, **36**, (3), pp. 1947–1960.
[25] Rajabi-Ghahnavieh, A., Fotuhi-Firuzabad, M., Othman, M.: 'Optimal unified power flow controller application to enhance total transfer capability'*IET Generation, Transmission & Distribution*, 2015, **9**, (4), pp. 358–368.
[26] Sadiq, A.A., Buhari, M., Adamu, S.S., Musa, H.: 'Coordination of multi-type FACTS for available transfer capability enhancement using PI–PSO'*IET Generation, Transmission & Distribution*, 2020, **14**, (21), pp. 4866–4877.
[27] El Moursi, M., Sharaf, A.M., El-Arroudi, K.: 'Optimal control schemes for SSSC for dynamic series compensation'*Electric Power Systems Research*, 2008, **78**, (4), pp. 646–656.
[28] 'SMARTVALVE™'. Available at https://www.smartwires.com/smartvalve
[29] Zhang, X.P., Rehtanz, C., Pal, B.: 'Flexible AC transmission systems: modelling and control' (Springer Science & Business Media, 2012)
[30] 'The Power Flow Equations'. Available at http://home.eng.iastate.edu/~jdm/ee553/DCPowerFlowEquations.pdf
[31] Sang, Y., Sahraei-Ardakani, M.: 'Effective power flow control via distributed FACTS considering future uncertainties'*Electric Power Systems Research*, 2019, **168**, pp. 127–136.
[32] Wiik, J.A., Takanori Isobe, Taku Takaku, *et al.*: 'Feasible series compensation applications using Magnetic Energy Recovery Switch (MERS)', Proc. 2007 European Conference on Power Electronics and Applications, Aalborg, Denmark, September 2007, pp. 1–9
[33] Wiik, J.A., Wijaya, F.D., Shimada, R.: 'Characteristics of the Magnetic Energy Recovery Switch (MERS) as a Series FACTS Controller'*IEEE Trans. Power Delivery*, 2009, **24**, (2), pp. 828–836.
[34] Gyugyi, L., Schauder, C.D., Williams, S.L., Rietman, T.R., Torgerson, D.R., Edris, A.: 'The unified power flow controller: a new approach to power transmission control'*IEEE Trans. Power Delivery*, 1995, **10**, (2), pp. 1085–1097.
[35] Guo, J., Crow, M.L., Sarangapani, J.: 'An Improved UPFC Control for Oscillation Damping'*IEEE Trans. Power Syst.*, 2009, **24**, (1), pp. 288–296.
[36] Fujita, H., Watanabe, Y., Akagi, H.: 'Control and analysis of a unified power flow controller'*IEEE Trans. Power Electron.*, 1999, **14**, (6), pp. 1021–1027.
[37] Noroozian, M., Angquist, L., Ghandhari, M., Andersson, G.: 'Use of UPFC for optimal power flow control'*IEEE Trans. Power Delivery*, 1997, **12**, (4), pp. 1629–1634.
[38] Sen, D., Acharjee, P.: 'Optimal line flows based on voltage profile, power loss, cost and conductor temperature using coordinated controlled UPFC'*IET Generation, Transmission & Distribution*, 2019, **13**, (7), pp. 1132–1144.
[39] Larsen, E.V., Clark, K., Miske, S.A., Urbanek, J.: 'Characteristics and rating considerations of thyristor controlled series compensation'*IEEE Trans. Power Delivery*, 1994, **9**, (2), pp. 992–1000.
[40] Paserba, J.J., Miller, N.W., Larsen, E.V., Piwko, R.J.: 'A thyristor controlled series compensation model for power system stability analysis'*IEEE Trans. Power Delivery*, 1995, **10**, (3), pp. 1471–1478.
[41] Glanzmann, G., Andersson, G.: 'Coordinated control of FACTS devices based on optimal power flow', Proc. 37th Annual North American Power Symposium, Ames, IA, USA, October 2005, pp. 141–148
[42] Shanmukha Sundar, K., Ravikumar, H.M.: 'Selection of TCSC location for secured optimal power flow under normal and network contingencies'*International Journal of Electrical Power & Energy Systems*, 2012, **34**, (1), pp. 29–37.
[43] Singh, J.G., Singh, S.N., Srivastava, S.C.: 'Enhancement of Power System Security through Optimal Placement of TCSC and UPFC', in '2007 IEEE Power Engineering Society General Meeting' 2007 IEEE Power Engineering Society General Meeting, (IEEE, 2007), pp. 1–6
[44] Duong, T., JianGang, Y., Truong, V.: 'A new method for secured optimal power flow under normal and network contingencies via optimal location of TCSC'*International Journal of Electrical Power & Energy Systems*, 2013, **52**, pp. 68–80.
[45] Gerbex, S., Cherkaoui, R., Germond, A.J.: 'Optimal location of multi-type FACTS devices in a power system by means of genetic algorithms'*IEEE Transactions on Power Systems*, 2001, **16**, (3), pp. 537–544.
[46] Shafik, M.B., Chen, H., Rashed, G.I., El-Sehiemy, R.A.: 'Adaptive Multi Objective Parallel Seeker Optimization Algorithm for Incorporating TCSC Devices into Optimal Power Flow Framework'*IEEE Access*, 2019, **7**, pp. 36934–36947.
[47] Papavasiliou, A., Oren, S.S., O'Neill, R.P.: 'Reserve Requirements for Wind Power Integration: A Scenario-Based Stochastic Programming Framework'*IEEE Transactions on Power Systems*, 2011, **26**, (4), pp. 2197–2206.
[48] Papavasiliou, A., Oren, S.S.: 'Multiarea Stochastic Unit Commitment for High Wind Penetration in a Transmission Constrained Network'*Operations Research*, 2013, **61**, (3), pp. 578–592.
[49] 'IBM CPLEX Optimizer'. Available at https://www.ibm.com/analytics/cplex-optimizer
[50] 'IPOPT Documentation'. Available at https://coin-or.github.io/Ipopt/
[51] 'BARON Solver'. Available at https://minlp.com/baron
[52] 'relative MIP gap tolerance'. Available at https://prod.ibmdocs-production-dal-6099123ce774e592a519d7c33db8265e-0000.us-south.containers.appdomain.cloud/docs/en/icos/12.8.0.0?topic=parameters-relative-mip-gap-tolerance
[53] Sahinidis, N.: 'BARON user manual v. 2021.1.13'. Available at https://www.minlp.com/downloads/docs/baron%20manual.pdf
[54] Birchfield, A.B., Xu, T., Gegner, K.M., Shetye, K.S., Overbye, T.J.: 'Grid Structural Characteristics as Validation Criteria for Synthetic Networks'*IEEE Trans. Power Syst.*, 2017, **32**, (4), pp. 3258–3265.
[55] 'ACTIVSg2000: 2000-bus synthetic grid on footprint of Texas'. Available at https://electricgrids.engr.tamu.edu/electric-grid-test-cases/activsg2000/
[56] 'Power System Test Case Archive - Reliability Test System (RTS)-1996'. Available at http://labs.ece.uw.edu/pstca/rts/pg_tcarts.htm
[57] Smart Wires Inc., 'SmartValve™ v1.04 Spec Sheet' (2021), pp. 1-3. Available at https://www.smartwires.com/download/20801/
[58] 'Power Systems Test Case Archive - 14 Bus Power Flow Test Case'. Available at https://labs.ece.uw.edu/pstca/pf14/pg_tca14bus.htm
[59] Matpower: 'Description of Case 14'. Available at https://matpower.org/docs/ref/matpower5.0/case14.html
[60] 'A Data Sheet for IEEE 14 Bus System'. Available at https://www.academia.edu/7781632/A_DATA_SHEETS_FOR_IEEE_14_BUS_SYSTEM

8. Appendix

Our method to increase the congestion level in the test systems is through reducing the capacity of lines. The modifications in the 2000-bus system are summarised in Table 9.

Table 9 Modifications of line capacities in the 2000-bus system

Line number	Capacity (MW)	Modified capacity (MW)
43	149	112
58	170	128
71	145	109

74	149	112
364	82	62
435	143.8	108
439	83	62
765	168	145
1038	150	113
1380	1450	1088
1381	1450	1088
2136	217.8	190
2382	1233	925
2389	220	165
2449	1600	1200
2450	1600	1200
2803	198	180
2911	280.8	220
2912	280.8	220
2913	280.8	220
2993	213	180
2994	213	180
2995	213	180

In the RTS-96 system, the capacity of line 23, which is the most utilised line in the system, is altered from 500 MW to 315 MW. For the rest of the lines in the system, the capacity is reduced by 10%.

Similarly, in the 14-bus system, the capacity of line 15 is reduced by 40%. For the rest of the lines in the system, the capacity is reduced by 10%.